

Immunological needles in the gene therapy haystack: applying a genetic paradigm to gene therapy

PR Lowenstein

Gene Therapy (2004) 11, 1–3. doi:10.1038/sj.gt.3302186

"I cannot promise to teach you all geology, I can only fire your imaginations." Adam Sedgwick; In: JW Clark and T Mc Hughes, *The Life and Letters of Adam Sedgwick*, 2 vols, Cambridge: Cambridge University Press, 1890, vol 2, p. 489; cited by Janet Browne in Charles Darwin, *Voyaging*, 1995, p. 139.

Replication-competent and replication-defective viral vectors have been developed as therapeutic options in cancer, infectious disorders, degenerative, metabolic, and genetic diseases. Still, immune responses against viral vectors play a crucial role in determining the long-term experimental and clinical effectiveness – and eventual fate – of viral vectors. To understand the phenomena responsible for the limitations imposed by the immune system on gene therapy, two approaches have been used. On the one hand, the direct consequences of injecting viral vectors into animals have been studied. These have determined that viral vectors induce the release of cytokines, interleukins, activate macrophages, induce T-cell and B-cell responses, induce viral-neutralizing antibodies, and induce the activation of the endothelium.^{1–6} Conversely, the role of many of these mechanisms has been tested in transgenic and knockout animals. These experiments have determined that the lack of complement, T cells, B cells, interleukins, interferons, and various methods used to downmodulate immune responses (CTLA4-Ig; sCD40L, etc) will prolong transgene expression in various tissues such as the liver, muscle, lung, or heart.^{7–9}

However, it remains difficult to determine which mechanisms regulate transgene longevity and which are epiphenomena.^{1–4} Two recent issues in *Gene Therapy Journals* have

been devoted to the mechanisms underlying immune responses to viral vectors.^{10,11} To identify the critical mechanisms, genetic approaches may provide the way forward by allowing a hypothesis-free search for those genes that direct the relevant immune responses to viral vectors.

In a very original paper published in this issue of *Gene Therapy*, Zhang *et al*¹² have applied genetic technologies to discover regions of the genome that may have a causal relationship to the longevity of adenovirus-mediated transgene expression in the liver. Specifically, they sought to determine the existence of quantitative trait loci (QTL) that linked to the longevity of transgene expression in the liver, the presence of cytotoxic T lymphocytes (CTLs) against adenovirus, and serum cytokines. A QTL is a restricted region of the genome that plays a role in the quantitative variation of the trait being studied; it is analyzed by correlating sequence variations in the genome with variations in traits that vary quantitatively in the population under study. Once identified, the QTL is most likely a polymorphism affecting protein function or the levels of protein expression.^{13–15}

To determine these QTL, they utilized 20 strains of recombinant inbred mice^{16–18} derived from a cross between C57BL/6J and DBA/2J;¹⁹ each recombinant inbred strain contains chromosomal regions that are derived from either parent, and they are homozygous at each locus (see Figure 1 for a schematic view of the production of recombinant inbred strains).

Liver β -galactosidase expression was measured for up to 50 days postinjection. At this stage, while some strains had lost >90% of liver β -galactosidase expression, in others

β -galactosidase expression was only reduced by <50%. Over the same time course, they measured parameters *a priori* linked to the longevity of transgene expression in the liver: serum levels IFN- γ , IL-6, and TNF- α , and levels of anti-adenovirus (CTLs).

Correlations were established between β -galactosidase expression in the liver and individual parameters measured in the 20 different recombinant inbred strains. The authors found a very strong and statistically significant correlation of the expression of β -galactosidase and the level of anti-adenovirus CTLs, while there was no correlation between the liver expression of β -galactosidase and serum levels of IFN- γ , TNF- α , or IL-6.

Statistical analysis was then used to compare the distribution of fairly evenly spaced chromosomal microsatellite markers throughout the genome of the strains studied, and each of the quantitative traits under evaluation (eg CTLs, cytokines, etc). Statistically significant QTLs represent areas of the genome whose presence correlates with the particular phenotype under consideration, for example, CTL. QTLs determined at long times post-virus administration reflect the capacity to clear β -galactosidase expression from the liver; this QTL mapped to Chr 15 at 42.8 cM, and Chr 19 at 33 cM. A QTL for CTL activity was identified on Chr 7 at 41 cM, and between 57.4 and 65.2, and on Chr 15 at 61.7 cM, and Chr X at 27.8 cM. QTLs for cytokine levels were also detected. While their levels correlated with each other, they did not correlate with either β -galactosidase clearance from the liver, or the presence of CTLs against adenovirus-infected cells.

We have learned from this paper that the host immune responses that regulate the longevity of adenovirus-mediated transgene expression in the liver is a polygenetic trait. The genetic determinants of this response can be studied in a statistically stringent manner, that may determine such immune responses, particular regions of the genome that may determine such immune responses. Also, this paper demonstrates the existence of strong strain differences in transgene expression and immune responses, and suggests that this may also occur in other strains and species. The importance of this to clinical gene therapy, and as an

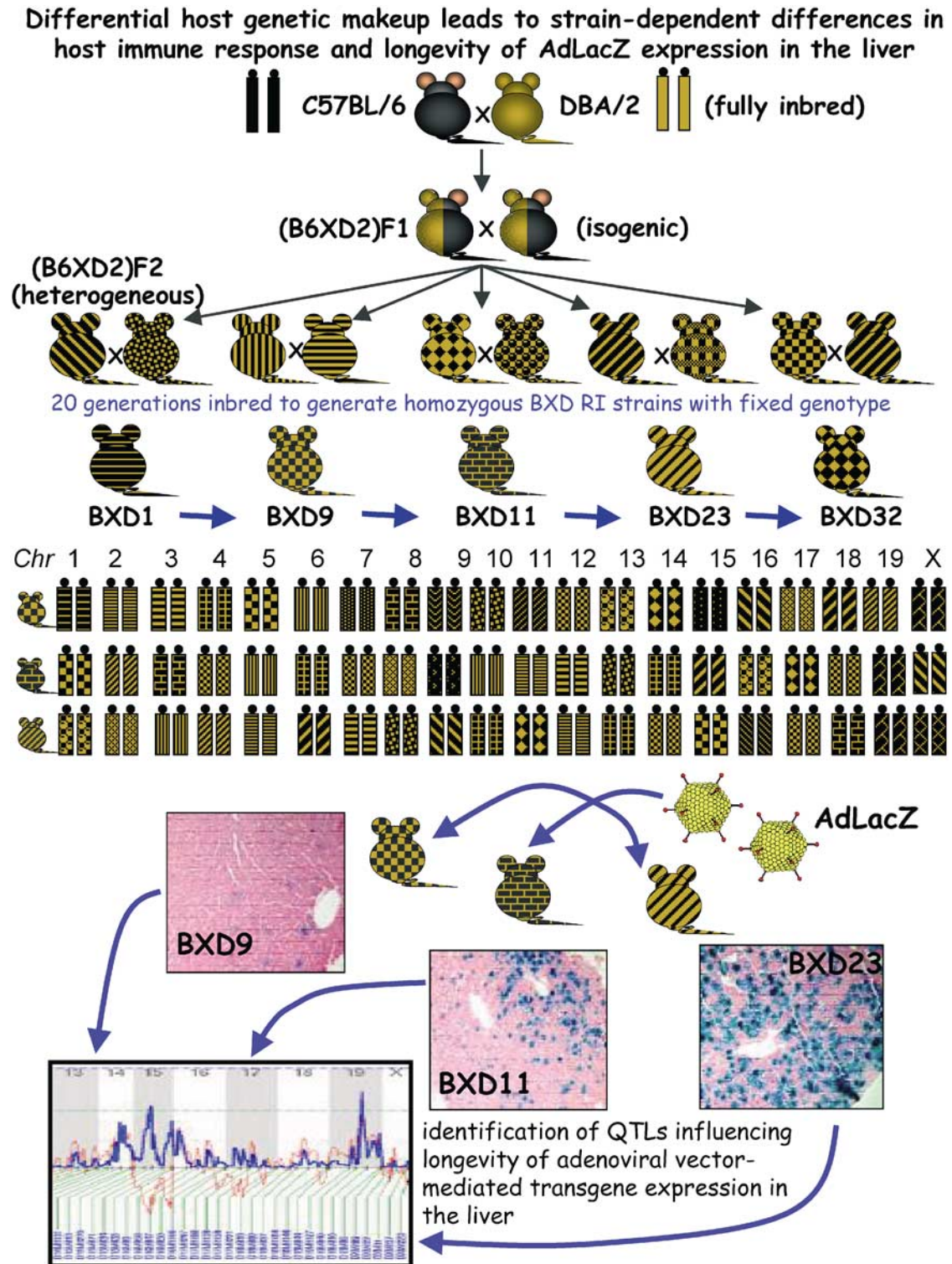


Figure 1 This figure summarizes the process involved in discovering QTLs determining anti-adenoviral immune responses eliminating vector-mediated β -galactosidase expression in the liver. The upper part of the figure illustrates how, from two inbred mouse strains, recombinant inbred strains (BXD1-BXD23) are generated by intercrossing F₂ mice for 20 generations. Each of the recombinant inbred strains are homozygous at each locus, as illustrated schematically for three strains in the middle of the figure. The lower third of the figure illustrates how adenovirus is then injected into all BXD recombinant inbred strains, and β -galactosidase expression, CTL levels, and cytokines are then measured. The correlation among different measurements is then performed and analyzed statistically. Longevity of transgene expression in the liver was only statistically correlated with levels of CTL. Genetic markers that are approximately evenly distributed throughout the mouse genome are then used to determine the variability of the genetic structure of each strain and compared to the variability of each measured response in the series of recombinant inbred mouse strains, and the results are then analyzed statistically. Statistically significant values indicate the location of potential QTL. Statistically significant QTL were identified for β -galactosidase expression, the level of CTLs, IFN- γ , TNF- α , and IL-6.

experimental model in which to test this variability is very high.

The next step will consist of identifying the sequence variations in the genome that contribute to each QTL. In spite of many recent advances in mouse genomic studies, this is a difficult task. One advantage of using the BXD recombinant inbred strains of mice is that the Mouse Genome Project will provide the complete sequence of the parental B6 and D2 genomes to interested investigators in the near future. Given that many of the polymorphic genes between B6 and D2 mice have been identified, the sequence of the BXD recombinant inbred strains will essentially be known. In the long run, the search aims to identify either a nucleotide polymorphism within the coding region that determines protein function, or a polymorphism within the promoter regions that affect the level of gene expression.^{13–18}

The power of the studies published is also necessarily limited to the QTLs defined *a priori*. Alternative hypotheses could propose, for example, that IFN- γ released by subtypes of immune cells directly in the liver contributes to clearing of adenovirus from the liver. Since these hypotheses have not been proposed, even though any of these may be of great importance, they have not been addressed in this manuscript. Importantly though, the same set of 20 recombinant inbred strains used in this work are available for the testing of any further hypothesis concerning the mechanisms of immune mechanisms that affect adenovirus vector-mediated transgene expression.

In summary, this paper represents an important advance in our capacity to examine and understand the molecular and genetic basis of the immune mechanisms that regulate viral vector-mediated transgene expression. To do so, much future hard work awaits its authors in narrowing down the QTL to a unique molecular basis. The possibility of identifying

those genes and their sequence variations that determine either the longevity of β -galactosidase expression or anti-adenoviral CTLs remains of great importance and general relevance to *Gene Therapy*.

Acknowledgements

I thank John Mountz for many challenging discussions, and joint preparation of Figure 1. ■

PR Lowenstein is at the Gene Therapeutics Research Institute, Cedars-Sinai Medical Center, Davis Bldg Room R5090, Beverly Blvd 8700, USA; and Department of Medicine, David Geffen School of Medicine, University of California Los Angeles, Los Angeles, CA, USA. PR Lowenstein is Bram and Elaine Goldsmith Chair in Gene Therapeutics. The support of the Board of Governors is kindly acknowledged. Work in my laboratory is funded by the National Institutes of Health. E-mail: lowensteinp@cshs.org

- 1 Yang Y, Wilson JM. Clearance of adenovirus-infected hepatocytes by MHC class I-restricted CD4+ CTLs *in vivo*. *J Immunol* 1995; **155**: 2564–2570.
- 2 Yang Y, Ertl HC, Wilson JM. MHC class I-restricted cytotoxic T lymphocytes to viral antigens destroy hepatocytes in mice infected with E1-deleted recombinant adenoviruses. *Immunity* 1994; **1**: 433–442.
- 3 Yang Y *et al*. Immune responses to viral antigens *versus* transgene product in the elimination of recombinant adenovirus-infected hepatocytes *in vivo*. *Gene Therapy* 1996; **3**: 137–144.
- 4 Yang Y, Li Q, Ertl HC, Wilson JM. Cellular and humoral immune responses to viral antigens create barriers to lung-directed gene therapy with recombinant adenoviruses. *J Virol* 1995; **69**: 2004–2015.
- 5 Chirmule N *et al*. Immune responses to adenovirus and adeno-associated virus in humans. *Gene Therapy* 1999; **6**: 1574–1583.
- 6 Molinier-Frenkel V *et al*. Immune response to recombinant adenovirus in humans: capsid components from viral input are targets for vector-specific cytotoxic T lymphocytes. *J Virol* 2000; **74**: 7678–7682.

- 7 Kafri T *et al*. Cellular immune response to adenoviral vector infected cells does not require *de novo* viral gene expression: implications for gene therapy. *Proc Natl Acad Sci USA* 1998; **95**: 11377–11382.
- 8 Amalfitano A, Parks RJ. Separating fact from fiction: assessing the potential of modified adenovirus vectors for use in human gene therapy. *Curr Gene Ther* 2002; **2**: 111–133.
- 9 Benihoud K *et al*. Efficient, repeated adenovirus-mediated gene transfer in mice lacking both tumor necrosis factor alpha and lymphotoxin alpha. *J Virol* 1998; **72**: 9514–9525.
- 10 Anderson WR. Adenoviral vector safety and toxicity. *Hum Gene Ther* 2002; **13**: 1–175.
- 11 Lowenstein PR. Immune responses to viral vectors for gene therapy. *Gene Therapy* 2003; **10**: 933–998.
- 12 Zhang HG *et al*. Identification of multiple genetic loci that regulate adenovirus gene therapy. *Gene Therapy* 2003; **11**: 4–14.
- 13 Moore KJ, Nagle DL. Complex trait analysis in the mouse: the strengths, the limitations and the promise yet to come. *Annu Rev Genet* 2000; **34**: 653–686.
- 14 Doerge RW. Mapping and analysis of quantitative trait loci in experimental populations. *Nat Rev Genet* 2002; **3**: 43–52.
- 15 Flint J, Mott R. Finding the molecular basis of quantitative traits: successes and pitfalls. *Nat Rev Genet* 2001; **2**: 437–445.
- 16 Williams RW, Gu J, Qi S, Lu L. The genetic structure of recombinant inbred mice: high-resolution consensus maps for complex trait analysis. *Genome Biol* 2001; **2**: 1–18.
- 17 Threadgill DW, Hunter KW, Williams RW. Genetic dissection of complex and quantitative traits: from fantasy to reality via a community effort. *Mamm Genome* 2002; **13**: 175–178.
- 18 Markel P *et al*. Theoretical and empirical issues for marker-assisted breeding of congenic mouse strains. *Nat Genet* 1997; **17**: 280–284.
- 19 Plomin R, McClearn GE, Gora-Maslak G, Neiderhiser JM. Use of recombinant inbred strains to detect quantitative trait loci associated with behavior. *Behav Genet* 1991; **21**: 99–116.

RESEARCH ARTICLE

Identification of multiple genetic loci that regulate adenovirus gene therapy

H-G Zhang^{1,2}, H-C Hsu¹, P-A Yang¹, X Yang¹, Q Wu¹, Z Liu¹, N Yi³ and JD Mountz^{1,2}¹Department of Medicine, Division of Clinical Immunology and Rheumatology, The University of Alabama at Birmingham, Birmingham, AL, USA; ²Veterans Administration Medical Center, Birmingham, AL, USA; and ³Section of Statistical Genetics, Department of Biostatistics, The University of Alabama at Birmingham, Birmingham, AL, USA

A key aspect of the immune response to adenovirus (Ad) gene therapy is the generation of a cytotoxic T-cell (CTL) response. To better understand the genetic network underlying these events, 20 strains of C57BL/6 × DBA/2 (BXD) recombinant inbred (RI) mice were administered with AdLacZ and analyzed at days 7, 21, 30, and 50 for liver β-galactosidase (LacZ) expression and CTL response. Sera levels of interferon gamma (IFN-γ), tumor necrosis factor-α (TNF-α), and interleukin-6 (IL-6) were analyzed at different times after AdLacZ. There was a distinct strain-dependent expression of LacZ, which was strongly correlated with the CTL response. Among the five BXD RI strains that exhibited significantly prolonged LacZ expression, four also exhibited a marked defect in the production of Ad-specific CTL. There

was a strong correlation between the sera levels of IFN-γ, TNF-α, and IL-6, but cytokine responses were not significantly correlated with LacZ expression or the CTL response. Quantitative trait loci regulating LacZ on day 30 were found on chromosome (Chr) 19 (33 cM) and Chr 15 (42.8 cM). Cytotoxicity mapped to Chr 7 (41.0 and 57.4–65.2 cM), Chr 15 (61.7 cM), and Chr X (27.8 cM). IFN-γ production mapped to Chr 18 (22, 27, and 32 cM) and Chr 11 (64.0 cM). TNF-α and IL-6 production mapped to Chr 6 (91.5 cM) Chr 9 (42.0 cM) and Chr 8 (52 and 73.0 cM). These results indicate that different strains of mice exhibit different pathways for effective clearance of AdLacZ depending on genetic polymorphisms and interactions at multiple genetic loci. Gene Therapy (2004) 11, 4–14. doi:10.1038/sj.gt.3302136

Keywords: adenovirus; cytotoxic T cells; genetic linkage analysis; BXD mice

Introduction

The immune response to adenovirus (Ad) has been a major factor limiting long-term Ad gene therapy and gene expression.^{1–3} The immune response also contributes to systemic toxicity and is one of the factors that limit the safety of gene therapy delivery.^{4,5} The development of helper-dependent Ad that lacks the entire Ad coding region results in a greatly decreased immune response and prolonged persistence of gene therapy.^{1,6} However, an antiviral immune response can still occur.⁷ One key aspect of the immune response is the generation of cytotoxic T cells (CTL).^{8–10} Inhibition of development of CTL has been achieved by blocking the Th1 helper T-cell response by immunosuppressive therapy,¹¹ anti-CD4 therapy^{12–14} anti-TNF therapy,¹⁵ and by therapies that block B7-CD28 signaling and CD40-CD40L interactions.^{16–20} We have previously developed cell-gene therapy utilizing either Fas ligand to delete specifically T cells responsive to Ad, or have blocked the hepatocyte to apoptosis with the soluble DR5, both of which result in prolonged gene therapy.^{21,22} Therefore, it is clear that crippling of one or more of the effector pathways of the

innate or adaptive immune response pathways to Ad gene therapy can greatly inhibit the elimination of Ad-infected hepatocytes and greatly prolong gene therapy expression. However, despite extensive knowledge of the different effector pathway mechanisms that contribute to elimination of the Ad gene therapy, the genetic basis of the immune response to Ad is not well understood.

We have previously used the C57BL/6 × DBA/2 (BXD) recombinant inbred (RI) strains of mice to dissect complex genetic loci that contribute to different aspects of the immune response, including thymic involution.^{23,24} Previous results by others²⁵ and us²⁶ have shown that BXD strains of mice exhibit differences in the CTL response and the induction of interferon gamma (IFN-γ) in response to tumors. A further advantage of utilizing these mice includes the possibility of identification of the genetic loci influencing the interested phenotype. Other investigators have used the BXD RI strains to determine the TNFα induced interleukin-6 (IL-6) response, and have mapped this to a locus on distal mouse chromosome (Chr) 12.²⁷ The genetic basis of the response to different viruses has been dissected using complex trait analysis and mouse genetic techniques. The immune response to mouse cytomegalovirus (MCMV) has been mapped to several loci on Chr 6 in a region that has recently been defined as the natural killer complex.^{28,29} Therefore, the BXD RI strains provide an ideal model to dissect genetic loci underlying the Ad immune response.

Correspondence: Dr JD Mountz, Department of Medicine, Division of Clinical Immunology and Rheumatology, The University of Alabama at Birmingham, 701 South 19th Street, LHRB 473, Birmingham, AL 35294, USA

Received 09 June 2003; accepted 19 July 2003

The present studies determine the genetic loci that control the immune response and clearance of LacZ from the liver after i.v. administration of AdLacZ. This is determined for cytokines including TNF- α , IL-6, and IFN- γ , as well as production of CTL. There was a distinct strain-dependent expression of LacZ, which was best correlated with the CTL response. The sera levels of TNF- α and IL-6 were strongly correlated with each other and also with IFN- γ . Genetic linkage analysis indicates that the LacZ expression was influenced by genetic loci on Chrs 19 and 15. The quantitative trait loci (QTL) associated with the CTL response were mapped to Chrs 7, 15, and X, whereas the production of cytokines was mainly influenced by QTL on Chrs 6, 8, 9, 11, and 18. Our results suggest that the chronic persistence of Ad vector in the host is influenced by multiple waves of genetic factors by the host.

Results

Strain-dependent expression of β -galactosidase in the liver

Liver β -galactosidase (LacZ) was determined by histologic staining and quantitative analysis was also carried out using a luminometer. Histologic analysis revealed that on day 21 after administration of LacZ, over one-half of the strains of mice exhibited very low expression of

LacZ in the liver, as represented by strain BXD9 (Figure 1a). Certain strains of BXD mice, including BXD strains 2, 8, 11, 16, and 23, exhibited either medium expression of β -galactosidase, represented by strain BXD11 (Figure 1a), or high expression of β -galactosidase, represented by strain BXD23 (Figure 1a). The β -galactosidase expression in the liver was quantitative in liver lysates using a luminometer (Figure 1b). The data points at days 7, 21, 30, and 50 are connected by a line for comparison of β -galactosidase in different BXD strains at the same time point. At day 7, most strains exhibited high expression of β -galactosidase. However, by day 21, over one-half of the strains exhibited greatly reduced expression of β -galactosidase. There were notable exceptions to this rapid decline in liver expression of β -galactosidase observed in strains 2, 8, 11, 16, and 23 (Figure 1b). By days 30 and 50, there continued to be high β -galactosidase expression in BXD strains 2, 11, 16, and 23 (Figure 1b). The strain distribution patterns (SDPs) of the AdLacZ expression on days 21, 30, and 50 exhibited a strong correlation with each other ($P < 0.0001$ for all comparisons).

High β -galactosidase correlates with low cytotoxic T-cell activity

To determine if differences in expression of β -galactosidase correlated with a difference in CTL response, the spleen T cells were isolated on days 7, 21, 30, and 50, and

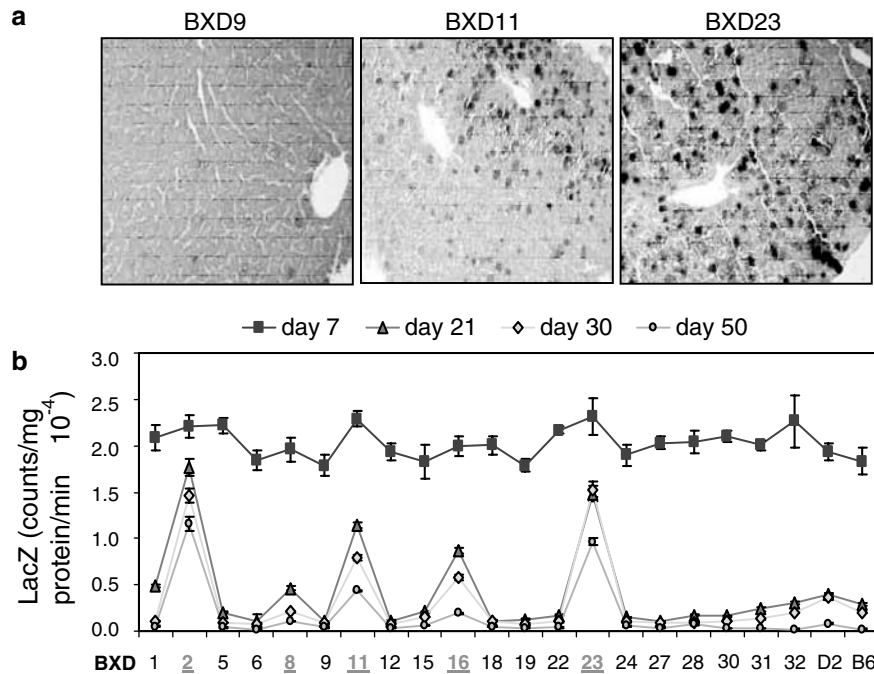


Figure 1 Differential AdLacZ expression in different BXD RI strains of mice. A total of 20 different BXD RI strains of mice, as well as parental D2 and B6 were injected i.v. with 5×10^9 PFU/mouse of AdLacZ. Mice (3–5 mice/group) were killed on days 7, 21, 30, and 50, after administration, and the liver was analyzed for AdLacZ expression. (a) Immunohistological staining of the liver tissue sections of a representative mouse of strain BXD9, BXD11, and BXD23 at day 30, after administration of AdLacZ. BXD strain 9 showed almost complete clearance of AdLacZ compared to persistent expression of AdLacZ in BXD11 and very low clearance of AdLacZ in BXD23. Magnification $\times 100$. (b) Liver tissue was homogenized, and LacZ was expression using a luminometer. LacZ expression was evaluated for three individual mice per strain at four different time points after administration of AdLacZ at day 7 (solid square), day 21 (upright triangle), day 30 (diamond), and day 50 (circle). The data points at days 7, 21, 30, and 50 are connected by a line for comparison of β -galactosidase in different BXD strains at the same time point. LacZ is expressed as counts per milligram of total liver protein per minute. The basal level of AdLacZ was 150 (0.015×10^4). The BXD strain number is shown below the expression level of β -galactosidase at different time points after administration of AdLacZ. The underlined strains in bold and underlined, strains 2, 8, 11, 16, and 23, as well as D2 indicate strains with significantly slow clearance of AdLacZ. The arrow bar represents the mean plus or minus standard error of the mean (s.e.m.) of three mice per group of each strain at each time point.

single-cell suspensions were prepared for use in CTL assays. There was a low CTL response in all strains of mice on day 7 after the AdLacZ administration (Figure 2a). However, there was a dramatic increase in this response on day 21 to day 30 in most strains of mice, which remained stable or declined slightly by day 50. The line is drawn for comparison of the CTL response in different BXD strains measured at the same time point. A high CTL response was correlated with rapid clearance of AdLacZ expression in these same strains of mice. However, the lower clearance of AdLacZ observed in BXD strain 2, 8, 11, 16, and 23 was correlated with a lower cytotoxicity response in these strains of mice. There was a significant correlation between the expression of LacZ and a low CTL response on days 21, 30, and

50, as illustrated for the day 30 time point ($R^2=0.65$, $P<0.0001$) (Figure 2b). The most profound defect in the CTL response was observed in BXD23, whereas BXD2, 8, 11, and 16 exhibited a similar cytotoxic response, despite differences in LacZ expression in these latter four strains.

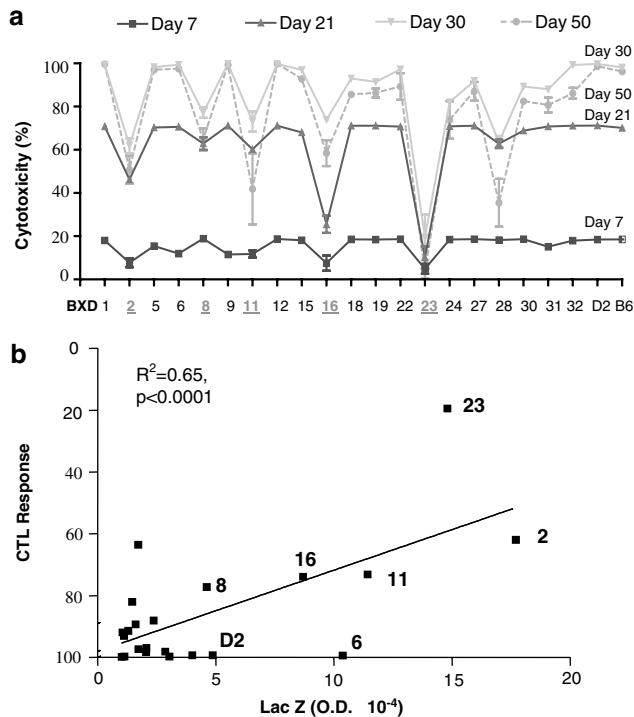


Figure 2 The CD8 CTL response correlates with clearance of AdLacZ. The CTL response was determined on days 7, 21, 30, and 50 after administration of AdLacZ (5×10^9 PFU/mouse) by killing the mice at the indicated time and preparing a single-cell suspension of the spleen. The spleen T cells were isolated on days 7, 21, 30, and 50, and single-cell suspensions were prepared and stimulated with MHC-compatible mouse embryonic fibroblasts (MEF) that had been transfected with Ad luciferase for use in CTL assays. For cytotoxicity assays, stimulated spleen T cells were incubated for 12 h with Ad luciferase (AdLuc) pulsed syngeneic MEF, and the cytotoxicity was determined by the percentage of cells that were lysed as determined by luciferase expression in the remaining cells. The luciferase activity was determined using a Top Count. (a) Cytotoxicity on day 7 (solid square), day 21 (upright triangle), day 30 (inverted triangle), and day 50 (solid circle). The line is drawn for comparison of the CTL response in different BXD strains measured at the same time point. The cytotoxicity varied from very low at early time points to almost 100% at later time points in most strains of mice. The BXD strain of mouse in which cytotoxicity was determined is shown below the cytotoxicity curve. The underlined strain shows the BXD RI strains with significantly lower cytotoxicity, which is evident especially on days 21 and 30, after administration of AdLacZ. (b) The cytotoxicity is plotted against LacZ. Each square represents the mean cytotoxicity at day 30 compared to the mean LacZ value at day 30. The number next to the squares represents BXD RI strains with significantly lower cytotoxicity or significantly higher LacZ expression at day 30.

QTLs that determine LacZ expression

The primary quantitative trait studied in these experiments, the expression of LacZ at different time points after administration of Ad, was determined on days 7, 21, 30, and 50. At day 7, after Ad administration, most of the strains expressed high LacZ, but there was an informative SDP even at this early time point. This SDP at day 7 most likely reflects Ad entry, initial expression or early clearance of AdLacZ in the liver. The suggestive QTLs associated with this initial susceptibility of the BXD RI strains to infection or production of LacZ were mapped to Chr 13 at 18 cM and to Chr 17 at 33.5 and 41.6 cM (Figure 3 and Table 1).

By days 21 and 30, there was high clearance of LacZ from the liver of most of the BXD RI strains of mice. However, there was a distinct SDP of LacZ clearance, and some strains of mice exhibited almost no expression of LacZ, whereas some strains of BXD RI mice exhibited relatively high expression of LacZ in the liver. On both days 21 and 30, the suggestive QTL that underlies the ability of the BXD RI strains to clear LacZ expression from the liver mapped to Chr 15 at 42.8 cM, and Chr 19 at 33 cM (Figure 3 and Table 1). The expressions of LacZ on days 21 and 30 were mapped independently, yet to the same two loci. This independent measurement of expression of LacZ in the liver of BXD RI strains of mice (three mice per group) at two different relatively late time points that map to the same QTL provides confidence in the reproducibility of the results, as well as in the significance of these QTLs for LacZ expression on Chrs 15 and 19.

QTLs associated with the cytotoxic T cell response mapped to Chrs 7, 15, and X

The CTL response was low on day 7 after administration of AdLacZ, and there was no QTL that reached a suggestive value for linkage. However, beginning on day 21 and also day 30, a distinct SDP of the CTL was evident. There was a very high correlation of the SDP of the CTL response at these time points (day 21 versus day 30, $R^2=0.75$, $P<0.0001$). Thus, the CTL response for days 21 and 30 yields an informative SDP for QTL analysis. The genetic linkage analysis on days 21 and 30 shows that the suggestive QTLs were mapped to Chr 7 at 41 cM and between 57.4 and 65.2 cM, Chr 15 at 61.7 cM, and Chr X at 27.8 cM (Figure 3 and Table 1). As with the LacZ expression QTLs, the quantitative trait of cytotoxicity was determined independently on days 21 and 30, after administration of AdLacZ. Both assays resulted in the suggestive QTLs at the same chromosome regions, again providing confidence with the reproducibility of the results.

Common mechanisms for cytokine production at the early stage are not correlated with AdLacZ or CTL response

In addition to the generation of CTL response, the production of cytokines has been shown to be an

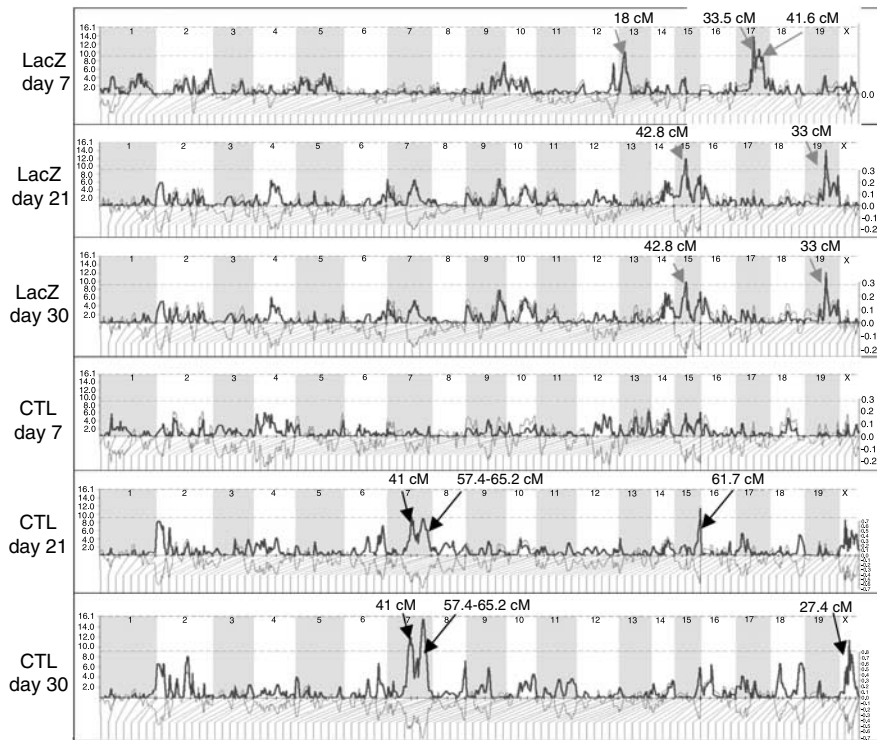


Figure 3 QTLs for LacZ and CTL. The QTLs for LacZ and CTL response at days 7, 21, and 30, after administration of AdLacZ, were determined using WebQTL. The results of WebQTL are shown for the entire mouse genome, including Chrs 1–19 and X. The chromosome number is indicated at the top of each compartment. The likelihood ratio statistic (LRS) value for each of the two traits at different days is plotted along each chromosome. The horizontal dashed line represents the threshold for suggestive QTLs. Three loci that reached a suggestive level of significance for LacZ expression at day 7 were found on Chr 13 at 18 cM and Chr 17 at 33.5 and 41.6 cM (indicated with arrows). Two different loci reached the suggestive level of significance for LacZ expression at days 21 and 30 on Chr 15 at 42.8 cM and Chr 19 at 33 cM (indicated with arrows). There were no QTLs that reached a suggestive level of significance for the CTL response at day 7. Two common QTLs for CTL response at days 21 and 30 were found on Chr 7 at 41 and 57.4–65.2 cM (indicated with arrows). QTLs for CTL response for days 21 and 30 were also found on Chr 15 (61.7 cM) and Chr X (27.8 cM), respectively. The lower grey line is an estimate of the additive effects of substituting a single *b* allele for *d* allele in the test interval.

Table 1 Summary of QTLs reaching suggestive value to influence AdLacZ expression and CTL response^a

	LacZ			CTL		
	Day 7	Day 21	Day 30	Day 7	Day 21	Day 30
Suggestive LRS	9.9	10.0	10.0	10.0	10.0	10.0
Significant LRS	17.8	17.9	17.9	18.7	17.9	17.6
QTL 1 ^a	<i>D17Mit274</i>	<i>D19Mit13^b</i>	<i>D19Mit13^b</i>	Undetected	<i>D15Mit35</i>	<i>DXMit25</i>
LRS	13.5	14.1	12.2	Undetected	11.6	11.4
Chromosome	17	19	19	Undetected	15	X
cM	33.5	33.0	33.0	Undetected	61.7	27.8
Positive allele ^c	D	D	D	Undetected	B	B
QTL 2 ^a	<i>D17Mit3</i>	<i>D15Mit29^b</i>	<i>D15Mit29^b</i>	Undetected	<i>D17Mit330 to D7Mit371^b</i>	<i>D17Mit330 to D7Mit371^b</i>
LRS	10.9	11.5	10.8	Undetected	10.1	16.0
Chromosome	17	15	15	Undetected	7	7
cM	41.6	42.8	42.8	Undetected	57.4–65.2	57.4–65.2
Positive allele ^c	D	B	B	Undetected	B	B
QTL 3 ^a	<i>D13Mit18</i>	Undetected	Undetected	Undetected	<i>D7Mit350^b</i>	<i>D7Mit350^b</i>
LRS	10.3	Undetected	Undetected	Undetected	10.0	10.3
Chromosome	13	Undetected	Undetected	Undetected	7	7
cM	18.0	Undetected	Undetected	Undetected	41.0	41.0
Positive allele ^c	D	Undetected	Undetected	Undetected	B	B

^aOnly QTLs greater than suggestive values are shown.

^bShaded QTLs are the ones that were detected for two different traits.

^cThe allele that contributes to an increase in trait value.

important factor that influences the clearance of Ad.^{15,30,31} Since the most dramatic decline in AdLacZ expression occurred between days 7 and 21 in all strains, except BXD, the sera levels of IFN- γ , TNF- α , and IL-6 were measured on days 7 and 14 after AdLacZ administration. The results again show a distinct SDP for cytokine production (Figure 4). Interestingly but not surprisingly, the levels of cytokines among mice of the same strain were all strongly correlated, and cytokine levels for IFN- γ at different time points were also correlated (Figure 5a). The highest correlation between cytokines was found comparing sera levels of TNF- α and sera levels IL-6 at day 7 (Figure 5b), followed by IFN- γ versus TNF- α (Figure 5c), and finally IFN- γ versus IL-6 (Figure 5d). However, the SDP of cytokine levels was not correlated with the SDP of AdLacZ expression or the SDP of the induction of CTL response. The discrepancy is especially apparent in BXD strains 2 and 23. Both these two strains had relatively high levels of LacZ and low levels of CTL response, yet the levels of cytokines were high in these two strains compared to many other strains of BXD mice (Figure 4).

The QTL associated with the induction of these cytokines after administration of Ad was determined using Map Manager QTX software^{32,33} and WebQTL program (<http://webqtl.roswellpark.org>).^{34,35} QTLs that reached a suggestive level of significance for IFN- γ were located on Chr 11 at 64.0 cM and Chr 18 at 22.0, 27.0, and 32 cM (Table 2 and Figure 6). QTLs that reached a suggestive level for TNF- α and IL-6 were found on Chr 8 at 52 and 73.0 cM and Chr 9 at 42.0 cM. A third QTL for IL-6, but not TNF- α , on Chr 6 at 41.5 cM reached a suggestive level of significance.

The similarities between the QTLs for TNF- α and IL-6 are consistent with the strong correlation between TNF- α and IL-6 (Figure 5b). In contrast, there is a lesser

correlation between the levels of IFN- γ and TNF- α or IFN- γ and IL-6, consistent with different QTLs that underlie production of IFN- γ compared to TNF- α and IL-6. The results are in agreement with results by Libert *et al*,²⁷ suggesting that same factors are involved in the production of TNF- α and IL-6 in BXD RI strains of mice.

Discussion

A hallmark for Ad vector evaluation *in vivo* is the persistence of transgene expression.^{5,36} Such persistence of transgene expression has therapeutic significance for treatment of chronic diseases such as tumors and autoimmune diseases. Most studies thus far have focused on the effect of deletion of Ad vector genome or the analysis of less immunogenic, syngeneic transgenes that minimize the immune response.^{1,6,7} Other studies have compared immune-competent versus immune-compromised manipulated hosts to better understand the biologic mechanisms involved in the immune response induced by Ad vectors.¹¹⁻²¹ Although such studies are crucial to understand the effects of isolated effector molecules on persistence of the Ad transgene, these studies are usually carried out in the same strain of mice, and cannot account for the genetic variability in the immune response in different strains of mice. Therefore, these studies may not be able to represent the various contributions of genetic polymorphisms to eliminate the administered Ad vectors, and thus prevent our understanding of the precaution and limitation of adenoviral gene therapy in immune diversified hosts such as humans.

Among the four immunological traits analyzed in this study that may be associated with the host immune response after Ad vector administration, we found that the host CTL response exhibited the best negative correlation with the Ad transgene expression. This correlation was largely due to a similar defect in the CTL response in BXD2, BXD11, and BXD16, and a more profound response in BXD23. The CTL response did not strongly correlate with the IFN- γ production, indicating that several factors influence the CTL response. The production of the innate immune response to Ad involves production of IFN- γ primarily by natural killer (NK) cells,^{22,31,37,38} and production of TNF- α primarily by Kupffer cells³⁹⁻⁴¹ can also be involved in eradicating the Ad-infected cells. There was a high correlation between the production of TNF- α and IL-6. There was also a significant, but lower correlation of the production of IFN- γ versus TNF- α and IL-6. Nevertheless, the production of these cytokines exhibited no significant correlation with the chronic expression of AdLacZ. This low correlation was particularly striking in BXD strains 2, 6, and 23. Transcriptional downmodulation of AdCMVLacZ has been associated with IFN- γ and TNF- α .⁴² We have carried out Ad genome analyses in several of the BXD RI and parental strains of mice, and the results indicate that the decrease in AdLacZ in these strains is indeed due to clearance of the Ad genome. In addition, the data indicate that the IFN- γ and TNF- α cytokine response does not correlate with the downregulation of LacZ. Together, these results indicate that downmodulation of AdLacZ in BXD mice is due to clearance of the AdLacZ viral genome and not due

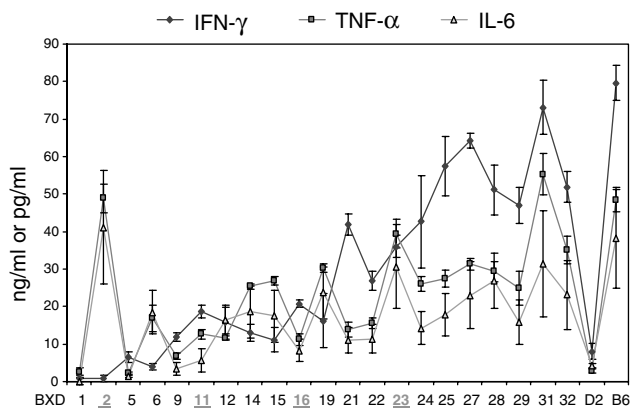


Figure 4 Cytokine production on day 7 after administration of AdLacZ. Sera collected from all strains of mice at day 7 after administration of AdLacZ were analyzed for expression of IFN- γ , TNF- α , and IL-6. The sera levels of IFN- γ are shown in ng/ml, and the sera levels of TNF- α and IL-6 are shown in pg/ml. These levels were determined using IFN- γ , TNF- α , or IL-6 standards in the ELISA assay. The numbers below the data points represent the individual BXD RI strain in which the sera levels of cytokines were evaluated. The values represent the mean \pm s.e.m. for IFN- γ (diamond), TNF- α (solid square), or IL-6 (open triangle). A line is drawn to connect the same cytokine in different BXD RI strains. Strains indicated with an underline were the ones with relatively high levels of LacZ on days 21, 30, and 50. Cytokine levels were not determined in BXD8.

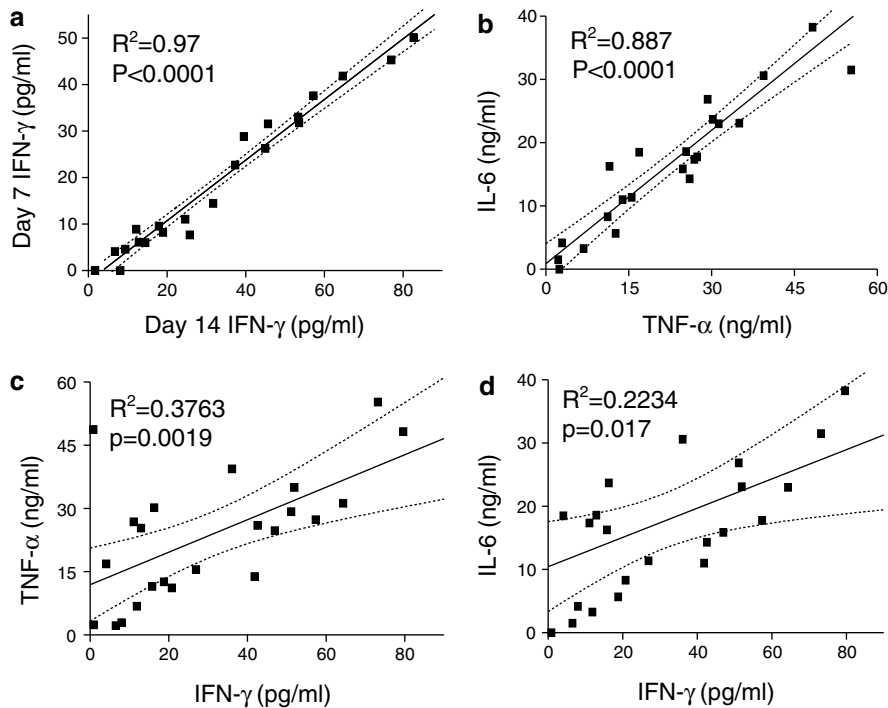


Figure 5 High correlation of TNF- α , IL-6, and IFN- γ in different BXD RI strains of mice. (a) Sera levels of IFN- γ at day 7 are plotted against sera levels of IFN- γ at day 14 in the different BXD RI strains of mice. Each square represents the mean of three determinations of IFN- γ in three different mice for each strain. The solid line represents a linear regression to the data points. The R^2 and P -value are shown on the graph. The 95% confidence interval for each straight line regression was determined and was shown as two dotted lines for each regression analysis. (b) Sera levels of TNF- α are plotted against sera levels of IL-6 in the different BXD RI strains of mice. Each square represents the mean of three determinations of TNF- α and IL-6 in three different mice for each strain at day 7. The solid line represents a linear regression to the data points, and the dash line represents the 95% confidence level curves. The R^2 and P -value are shown on the graph. (c) IFN- γ is plotted against TNF- α as described in (b). (d) IFN- γ is plotted against IL-6 as described in (b).

to silencing of the LacZ promoter. Thus, our results suggest that the host CTL response is the most important factor that determines the level of Ad transgene expression. However, we cannot exclude the possibility that some combination of the cytokines analyzed in these experiments, or analysis of additional cytokines, will correlate with LacZ expression. It is also possible that analysis of the temporal sequence of cytokine production, as well as a site of production, to provide a stronger correlation with LacZ expression. The present results suggest that the relationship between cytokine production and LacZ clearance is more complex than might be predicted from previous work in this field, including our own.^{13,15}

Since NK cells have been implicated in clearance of Ad, it is possible that the decreased LacZ clearance in BXD8 may be related to the mutation of the NK cell lectin-like receptor family 8 (*Klra8*) that is mutated in BXD8.^{28,29} *Klra8* (or *ly49h*) has been identified as a gene encoding an NK surface receptor that interacts with MHC class I molecules and can act to activate NK cells. The Ly49H receptor, located on Chr 6, directly recognizes an MCMV-encoded protein, m157, as the ligand, and the NK cell defect has been proposed to be specific for MCMV.⁴³ It is not known if the mutation of *ly49h* in BXD8 is a factor in defective clearance of LacZ.

To determine if the QTLs for the AdLacZ cytotoxic response correlated with other QTLs previously reported for T-cell responses, we searched the Mouse Genome Informatics website (www.informatics.jax.org).^{44,45} The

AdLacZ CTL locus *D7Mit350* (Chr 7, 41 cM) is close to a previously mapped T-cell receptor-induced activation 4 (*Tira 4*) locus at *D7Mit32* (37 cM) that is associated with the T-cell proliferative response after anti-CD3 stimulation.⁴⁶ The AdLacZ CTL locus between *D7Mit330* and *D7Mit371* (Chr 7, 57.4–65.2 cM) is close to the genetic locus associated with the CD8 T-cell response against murine leukemia virus infection previously identified by Panoutsakopoulou *et al.*⁴⁷ Thus, both these two studies support the finding in this report that a telomeric region on mouse Chr 7 harbors genes regulating the Ad-induced CD8 CTL response.

A Phenome database has been established for the BXD RI strains, and can be accessed at WebQTL (www.webqtl.org).³⁴ Therefore, it was possible to correlate the SDP we observed for AdLacZ expression, CTL response, TNF- α , IFN- γ , and IL-6 with the SDP reported by other investigators. Using this approach, we observed that the SDP for AdLacZ-induced TNF- α and IL-6 correlated with the SDP previously reported for TNF- α -induced body temperature loss ($R=-0.63$) and TNF- α -induced serum IL-6 ($R=-0.46$).²⁷ However, the QTLs influencing the sera levels of TNF- α and IL-6 in the present study have been identified to be on mouse Chrs 6, 8, and 9, but not on Chr 12 as in the previous report.²⁷ Using the mouse genome informatics website, the common QTL regulating IL-6 and TNF- α (Chr 9, 42 cM) after AdLacZ was found to be close to a previous QTL on Chr 9 (35 cM) associated with both the inflammatory response and arthritis induced by proteoglycan in

Table 2 Summary of QTLs reaching suggestive value to influence cytokine production^a

	Day 7		
	IFN- γ	TNF- α	IL-6
Suggestive LRS	10.1	9.8	9.6
Significant LRS	18.4	16.7	16.7
QTL 1 ^a	<i>D18Mit53</i>	<i>Tcf12</i> ^b	<i>D8Mit113</i> ^b
LRS	10.7	12.3	12.2
Chromosome	18	9	8
cM	27.0	42.0	52.0
Positive allele ^c	B	B	B
QTL 2 ^a	<i>D18Mit17</i>	<i>D8Mit156</i> ^b	<i>D6Mit67</i>
LRS	10.2	11.2	11.1
Chromosome	18	8	6
cM	22.0	73.0	41.5
Positive allele ^c	B	B	B
QTL 3 ^a	<i>D18Mit124</i>	<i>D8Mit113</i> ^b	<i>D8Mit156</i> ^b
LRS	10.2	9.9	11.7
Chromosome	18	8	8
cM	32.0	52.0	73.0
Positive allele ^c	B	B	B
QTL 4 ^a	<i>D11Mit360</i>	Undetected	<i>Tcf12</i> ^b
LRS	10.2	Undetected	10.8
Chromosome	11	Undetected	9
cM	64.0	Undetected	42.0
Positive allele ^c	B	Undetected	B

^aOnly QTLs greater than suggestive values are shown.

^bShaded QTLs are the ones that were detected for two different traits.

^cThe allele that contributes to an increase in trait value.

(BALB/c \times DBA/2)F₂ mice⁴⁸ and also the duration and onset of experimental allergic encephalomyelitis in (SJL/J \times B10.S/DvTe)F₂ mice.⁴⁹ Similarly, the QTL influencing IL-6 on Chr 6 (41.5 cM) is close to a previously mapped QTL on Chr 6 (44 cM) for autoimmune gastritis,⁵⁰ collagen II-induced arthritis (Chr 6, 48.7 cM),⁵¹ and cutaneous hypersensitivity (Chr 6, 45.5 cM).⁵² These results suggest that these regions on mouse Chrs 9 and 6 contain a gene or a cluster of genes that not only influence the proinflammatory response to Ad, but also other inflammatory processes in mice.

In summary, our results suggest that, in the majority of BXD RI strains of mice, the major factors that determine the duration of Ad transgene expression occurred at late time points following AdLacZ administration. The levels of TNF- α and IL-6 are closely associated with each other but are not correlated with the final level of AdLacZ. The CTL response exhibited the best correlation with the expression of AdLacZ and may be directly associated with the prolonged Ad transgene expression. Thus, despite the host immune heterogeneity, our results strongly indicate that the regulation of the host CTL response is the major consideration for improving the duration of the Ad-induced transgene expression.

Methods

Mice and treatments

Female C57BL/6J (B6), DBA/2J (D2), and RI BXD/Ty mice were provided by the UAB Facility of Genetic Mapping of Complex Trait in the Mouse. The strains of BXD RI mice used are BXD1, BXD2, BXD5, BXD6, BXD8, BXD9, BXD11, BXD12, BXD15, BXD16, BXD18, BXD19,

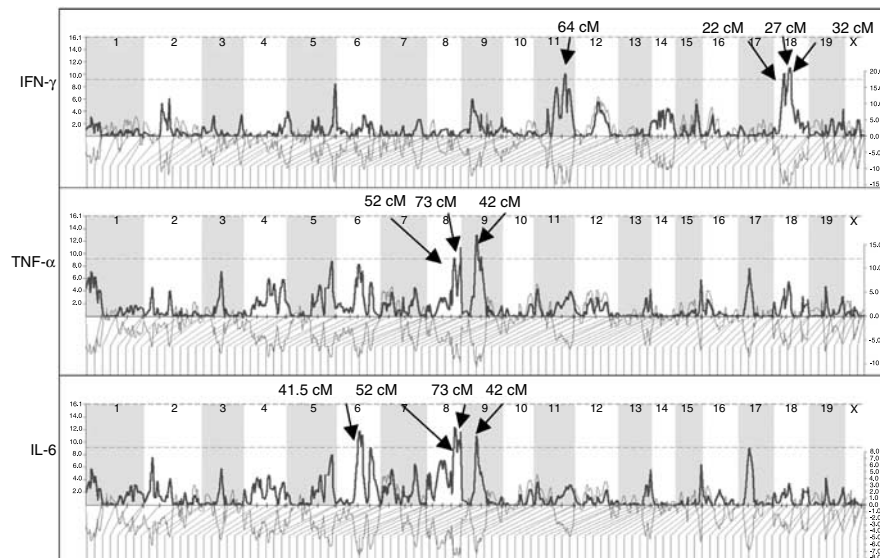


Figure 6 QTL analysis for IFN- γ , TNF- α , and IL-6. The levels of these cytokines on day 7 after AdLacZ administration were used to determine the significant QTLs. QTLs were determined using the Map Manager QTX and the WebQTL software. The QTLs for the entire genome from Chrs 1–19 and Chr X are shown. The number of each chromosome is indicated on the top of each compartment. The dashed lines indicate the threshold for suggestive QTLs. There were four suggestive QTLs for IFN- γ on Chr 11 at 64 cM and Chr 18 at 22, 27, and 32 cM. There were three identical QTLs for TNF- α and IL-6, on Chr 8 at 52 and 73 cM and on Chr 9 at 42 cM. There was also a fourth QTL for IL-6 production on Chr 6 at 41.5 cM that reached a suggestive value. The lower grey line is an estimate of the additive affects of substituting a single b allele for d allele in the test interval.

BXD22, BXD23, BXD24, BXD27, BXD28, BXD30, BXD31, and BXD32. Mice were kept in micro-isolators and were fed with sterilized food and water *ad libitum* until they were killed at days 7, 21, 30, and 50 after treatment with AdLacZ (5×10^9 PFU/mouse) using i.v. injection. Three mice from each group were sampled at each time point for analysis of LacZ and CTL. All experiments conducted in this study have been reviewed and approved by the Institutional Animal Care and Use Committee (IACUC) of the University of Alabama at Birmingham.

Production of recombinant AdCMVLacZ

A recombinant E1 detected serotype 5 Ad expressing β -galactosidase (AdLacZ) was constructed as described previously.^{15,22} To obtain a large quantity of recombinant AdLacZ, 293 cells were infected and grown for 40 h at 37°C prior to harvest and centrifugation using a table-top centrifuge at 4000 rpm for 20 min. The infected cells were resuspended in PBS buffer, then lysed using three freeze-thaw cycles. The released virus was purified through two cesium chloride gradients and then the purified recombinant AdLacZ was titrated by a plaque assay as described previously,¹⁵ aliquoted and stored at -80°C until used.

Expression of LacZ in the liver

Hepatic expression of LacZ was determined in different treatment groups by killing mice at days 7, 21, 30, and 50 and stained with β -Gal, as previously described.^{15,22} In brief, the frozen sections were fixed in fresh 4% paraformaldehyde in PBS for 1 h at 4°C, rinsed, and stained with 0.1% X-gal, 5 mM $K_3Fe(CN)_6$, and 5 mM $K_4Fe(CN)_6$ for 24 h at 25°C in dark room overnight. β -galactosidase activity in the liver lysate was measured using the Galacto-light β -galactosidase detection kit (Tropix Inc., Bedford, MA, USA). Briefly, 100 mg of liver was homogenized in 1 ml of lysis solution. The lysis solution was prepared by addition of 10 μ l of a 0.1 M solution of dithiothreitol, 1 μ l of 30% hydrogen peroxide, and 100 μ l of protease inhibitor mixture (Complete, Roche Molecular Biochemicals, Indianapolis, IN, USA). The protein concentration of the lysate was determined, and 100 μ g of lysate was used for quantitation of β -galactosidase activity. Recombinant β -galactosidase (Sigma, St Louis, MO, USA) was used as a positive control, and liver lysate from nontransfected mice was used as a negative control. The final reaction mixture containing light-emitting substrates was measured using a luminometer (Wallace Incorporated, Gaithersburg, MD, USA) and the results of the β -galactosidase activity were calculated as counts/mg of total liver protein/min.

Cytotoxic T-cell response analysis

CTL response analysis was performed using a bioluminescence assay as previously described, except that the β -galactosidase reporter substrate was replaced by luciferase.⁵³ Briefly, Ad luciferase (AdCMVLuc)-infected MHC-compatible mouse embryonic fibroblasts (MEFs) (50 PFU/cell) were cocultured with effector T cells at different ratios. These effector T cells were obtained from mice injected with AdLacZ at day 0, and killed at days 7, 21, 30, and 50, as described for LacZ analysis. Single-cell suspension from the spleen of mice (3–5 mice per group) was produced as described previously and stimulated with γ -irradiated MHC-compatible fibroblasts

transfected with AdCMVLuc (10 PFU/cell) for 4 days at 37°C in a CO₂ incubator. For cytotoxicity assays, the stimulated T cells from the different BXD RI strains of mice were incubated with the Ad-luciferase-transfected MEFs for 12 h at different ratios of effector (E) to target (T) cells. The % of viable cells was determined by analysis of the remaining luciferase activity using a luciferase assay kit (Promega, Madison, WI, USA) and counted using a Top Count.⁵⁴ Cytotoxicity was calculated as (100-% viability). The maximum luciferase response (100% viability) was determined using transfected MEFs without T cells and minimum luciferase response (0% viability) was determined using untransfected MEFs.

Analysis of serum levels of IL-6, TNF- α , and IFN- γ

Blood samples were collected at different times after treatments, and the serum levels of IL-6, TNF- α , and IFN- γ were measured by an ELISA kit for mouse IL-6, TNF- α , or IFN- γ (BioSource International, Inc., Camarillo, CA, USA).

Genotype of BXD RI mice

The current mapping data files for BXD RI strains were generated by Williams *et al*^{55,56} and Taylor *et al*.⁵⁷ Genomic DNA of each BXD RI strain was extracted from the spleen using a high-salt procedure.⁵⁸ A total of 938 primer pairs (MapPairs) that selectively amplify polymorphic MIT microsatellite loci distributed across all autosomes and the X chromosome between B6 and D2 strains of mice (Research Genetics, Huntsville, AL, USA) were typed using a modified version of the PCR protocol of Dietrich *et al*⁵⁹ and described in detail at Dr Robert Williams website (<http://www.nervenet.org>).⁵⁵ The complete BXD RI genotype data set genotyped using the method described above was provided by Dr Williams at the University of Tennessee (Memphis). This data set can be downloaded from the website of Neurogenetics at UT Health Science Center (<http://www.nervenet.org>). All loci with redundant SDPs were purged, leaving a final BXD RI genotype marker set of approximately 620 unique nonredundant markers.

Databases

A summary of information on chromosomal positions of the MIT microsatellite markers was obtained from the Portable Dictionary of the Mouse Genome (<http://www.nervenet.org/fmpfiles/fmplist.html>)^{55,56} and the MIT/Whitehead SSLP database (<http://www-genome.wi.mit.edu/snp/mouse/>).⁶⁰ Additional databases devoted to previously mapped QTLs and polymorphic genes and markers between B6 and D2 strains of mice were obtained from the Mouse Genome Database (www.jax.org).^{44,45} Relational database files between different phenotypes measured using BXD RI strains of mice are available from the WebQTL (<http://webqtl.roswellpark.org>).^{34,35}

Statistics of genetic linkage analysis

Loci with log of the odds ratio (LOD) scores greater than ~ 2.8 ($P < 1.6 \times 10^{-3}$) and 4.3 ($P < 5.2 \times 10^{-5}$) were considered suggestive and significant, respectively.⁶¹ Chromosomes harboring suggestive loci were analyzed by simple interval mapping. Genome-wide (experiment-wise) significance probabilities for mapped QTLs were estimated by comparing peak likelihood ratio statistics

(LRSs) ($LRS = LOD \times 4.6$) of correctly ordered data sets with those computed for 10 000 permutations of the phenotype data.⁶² Probabilities reported below as 'genome-wide' (P_G) reflect correction for multiple tests; other reported probabilities are comparison-wise. Confidence of QTL position is given as the 2-LOD support interval that bounds the QTL with ~95% confidence.⁶³

Quantitative trait loci analysis

The values were analyzed using the software program MapManager QTX (KF Manley, mapmgr@mcbio.med.buffalo.edu, Buffalo, NY, USA)^{32,33} and WebQTL (<http://webqtl.roswellpark.org>)^{34,35} to conduct a genome-wide search for mapping QTLs. In this case, the user is not required to discriminate between 'B' and 'D' phenotypes. Rather, the quantitative phenotypic data for each RI strain serve as the starting point for analysis. This results in statistics that are essentially two-tailed, more conservative than may be warranted in some situations with extreme differences between parental lines. Irrespective of the complexity, the strategy for mapping is to discover the most similar, if not identical, SDP from the large list of genotypes mapped in BXD strains. A concordance between a phenotypic SDP and an existing genotypic SDP (map location) indicates the presence of a QTL at or near that location contributing to the phenotype. However, due to the limited number of BXD strains available, the number of SDPs to be compared, and consequently the complexity of testing required to establish concordance, a close match in SDPs may occur by chance.^{62,64} As with all statistical comparisons, it is necessary to make a calculation of the probability that the observed result was a false positive. We therefore have calculated the genome-wide probability of obtaining the observed linkages by random chance corresponding to an error threshold of $P=0.05$, that is, one chance in 20 of such a false-positive error. We did this using a nonparametric permutation method developed by Churchill and Doerge,⁶² which is implemented in the Map Manager QTX software³³ and WebQTL program (<http://webqtl.roswellpark.org>).^{34,35}

Interval mapping

A subroutine of the Map Manager QTX software³³ and WebQTL (<http://webqtl.roswellpark.org>),^{34,35} using computationally efficient regression equations, has been used for mapping the QTLs.^{32,33,62} The probability of linkage between our traits and previously mapped genotypes was estimated at 1-cM intervals along the entire genome, except for the Y chromosome. The statistical power of linkage of the phenotype to individual genotypes (point-wise linkage statistics) that attained values of between 0.0001 and 0.00002 was considered to have reached a level of genome-wide statistical significance. Linkages approximating that level are deemed 'suggestive' and are worthy of reporting, although confirmation of linkage is required.⁶² To establish criteria for suggestive and significant linkage, a permutation test is performed using MapManager QTX (>5000 permutations at 1 cM intervals).⁶² This test compares the peak LRS score obtained for a given data set with the peak LRS obtained for 1000 random permutations of the same data set. The latest iteration of Map Manager allowed us to apply a weighted least-

square regression model, which resulted in a greater power and precision in mapping QTLs.

Acknowledgements

We thank Ms Carol Humber for excellent secretarial work. This work was supported by NIH Grants R01 AG 16653, N01 AR 6-2224, RO1 AI 42900, and CA 20408, and a Birmingham VAMC Merit Review Grant. Huang-Geng Zhang is a recipient of Arthritis Foundation Investigator Award.

References

- Liu Q, Muruve DA. Molecular basis of the inflammatory response to adenovirus vectors. *Gene Therapy* 2003; **10**: 935–940.
- Chirmule N *et al*. Immune responses to adenovirus and adeno-associated virus in humans. *Gene Therapy* 1999; **6**: 1574–1583.
- Michou AI *et al*. Adenovirus-mediated gene transfer: influence of transgene, mouse strain and type of immune response on persistence of transgene expression. *Gene Therapy* 1997; **4**: 473–482.
- St George JA. Gene therapy progress and prospects: adenoviral vectors. *Gene Therapy* 2003; **10**: 1135–1141.
- Wickham TJ. Targeting adenovirus. *Gene Therapy* 2000; **7**: 110–114.
- Parks R, Eveleigh C, Graham F. Use of helper-dependent adenoviral vectors of alternative serotypes permits repeat vector administration. *Gene Therapy* 1999; **6**: 1565–1573.
- Roth MD *et al*. Helper-dependent adenoviral vectors efficiently express transgenes in human dendritic cells but still stimulate antiviral immune responses. *J Immunol* 2002; **169**: 4651–4656.
- Yang Y, Li Q, Ertl HC, Wilson JM. Cellular and humoral immune responses to viral antigens create barriers to lung-directed gene therapy with recombinant adenoviruses. *J Virol* 1995; **69**: 2004–2015.
- Yang Y, Wilson JM. Clearance of adenovirus-infected hepatocytes by MHC class I-restricted CD4+ CTLs *in vivo*. *J Immunol* 1995; **155**: 2564–2570.
- Kim M, Kim K. Diversity and complexity of CD8+ T cell responses against a single epitope of adenovirus E1B. *Virology* 2002; **295**: 238–249.
- Cichon G, Strauss M. Transient immunosuppression with 15-deoxyspergualin prolongs reporter gene expression and reduces humoral immune response after adenoviral gene transfer. *Gene Therapy* 1998; **5**: 85–90.
- Ye X *et al*. Transient depletion of CD4 lymphocyte improves efficacy of repeated administration of recombinant adenovirus in the ornithine transcarbamylase deficient sparse fur mouse. *Gene Therapy* 2000; **7**: 1761–1767.
- Minter RM *et al*. TNF-alpha receptor signaling and IL-10 gene therapy regulate the innate and humoral immune responses to recombinant adenovirus in the lung. *J Immunol* 2000; **164**: 443–451.
- Shean MK *et al*. Immunomodulation and adenoviral gene transfer to the lungs of nonhuman primates. *Hum Gene Therapy* 2000; **11**: 1047–1055.
- Zhang HG *et al*. Inhibition of tumor necrosis factor alpha decreases inflammation and prolongs adenovirus gene expression in lung and liver. *Hum Gene Ther* 1998; **9**: 1875–1884.
- Yang Y, Wilson JM. CD40 ligand-dependent T cell activation: requirement of B7-CD28 signaling through CD40. *Science* 1996; **273**: 1862–1864.
- Schwalter DB *et al*. Constitutive expression of murine CTLA4Ig from a recombinant adenovirus vector results in prolonged transgene expression. *Gene Therapy* 1997; **4**: 853–860.

- 18 Scaria A *et al.* Antibody to CD40 ligand inhibits both humoral and cellular immune responses to adenoviral vectors and facilitates repeated administration to mouse airway. *Gene Therapy* 1997; **4**: 611–617.
- 19 Guerette B *et al.* Prevention of immune reactions triggered by first-generation adenoviral vectors by monoclonal antibodies and CTLA4Ig. *Hum Gene Ther* 1996; **7**: 1455–1463.
- 20 Ziller C, Stoeckel F, Boon L, Haegel-Kronenberger H. Transient blocking of both B7.1 (CD80) and B7.2 (CD86) in addition to CD40–CD40L interaction fully abrogates the immune response following systemic injection of adenovirus vector. *Gene Therapy* 2002; **9**: 537–546.
- 21 Zhang HG *et al.* Induction of specific T-cell tolerance by adenovirus-transfected, Fas ligand-producing antigen presenting cells. *Nat Biotechnol* 1998; **16**: 1045–1049.
- 22 Zhang HG *et al.* Hepatic DR5 induces apoptosis and limits adenovirus gene therapy product expression in the liver. *J Virol* 2002; **76**: 5692–5700.
- 23 Hsu HC *et al.* Age-related change in thymic T-cell development is associated with genetic loci on mouse chromosomes 1, 3, and 11. *Mech Ageing Dev* 2002; **123**: 1145–1158.
- 24 Hsu H-C *et al.* Age-related thymic involution in C57BL/6J × DBA/2J recombinant inbred mice maps to mouse chromosomes 9 and 10. *Genes Immun* 2003, (in press).
- 25 Schirmacher V, Landolfo S, Zawatzky R, Kirchner H. Immunogenetic studies on the resistance of mice to highly metastatic DBA/2 tumor cell variants. II. Influence of minor histocompatibility antigens on tumor resistance, gamma-interferon induction and cytotoxic response. *Invasion Metastasis* 1981; **1**: 175–194.
- 26 Grizzle WE *et al.* BXD recombinant inbred mice represent a novel T cell-mediated immune response tumor model. *Int J Cancer* 2002; **101**: 270–279.
- 27 Libert C *et al.* Identification of a locus on distal mouse chromosome 12 that controls resistance to tumor necrosis factor-induced lethal shock. *Genomics* 1999; **55**: 284–289.
- 28 Lee SH *et al.* Susceptibility to mouse cytomegalovirus is associated with deletion of an activating natural killer cell receptor of the C-type lectin superfamily. *Nat Genet* 2001; **28**: 42–45.
- 29 Scalzo AA *et al.* The effect of the Cmv-1 resistance gene, which is linked to the natural killer cell gene complex, is mediated by natural killer cells. *J Immunol* 1992; **149**: 581–589.
- 30 Vassalli G. Gene therapy of heart transplantation. *Rev Med Suisse Romande* 2002; **122**: 145–148.
- 31 Acsadi G *et al.* Interferons impair early transgene expression by adenovirus-mediated gene transfer in muscle cells. *J Mol Med* 1998; **76**: 442–450.
- 32 Manly KF, Olson JM. Overview of QTL mapping software and introduction to map manager QT. *Mamm Genome* 1999; **10**: 327–334.
- 33 Manly KF, Cudmore Jr RH, Meer JM. Map Manager QTX, cross-platform software for genetic mapping. *Mamm Genome* 2001; **12**: 930–932.
- 34 Chesler EJ *et al.* Genetic correlates of gene expression in recombinant inbred strains: a relational model to explore for neurobehavioral phenotypes. *Neuroinformatics* 2003, (in press).
- 35 Wang J, Williams RW, Chesler EJ, Manly KF. WebQTL: web-based complex trait analysis. *Neuroinformatics* 2003, (in press).
- 36 Benihoud K, Yeh P, Perricaudet M. Adenovirus vectors for gene delivery. *Curr Opin Biotechnol* 1999; **10**: 440–447.
- 37 Burgert HG *et al.* Subversion of host defense mechanisms by adenoviruses. *Curr Top Microbiol Immunol* 2002; **269**: 273–318.
- 38 Peng Y, Falck-Pedersen E, Elkon KB. Variation in adenovirus transgene expression between BALB/c and C57BL/6 mice is associated with differences in interleukin-12 and gamma interferon production and NK cell activation. *J Virol* 2001; **75**: 4540–4550.
- 39 Doerschug K *et al.* First-generation adenovirus vectors shorten survival time in a murine model of sepsis. *J Immunol* 2002; **169**: 6539–6545.
- 40 Wheeler MD *et al.* Adenoviral gene delivery can inactivate Kupffer cells: role of oxidants in NF-kappaB activation and cytokine production. *J Leukoc Biol* 2001; **69**: 622–630.
- 41 Matsuki Y *et al.* Soluble Fas gene therapy protects against Fas-mediated apoptosis of hepatocytes but not the lethal effects of Fas-induced TNF-alpha production by Kupffer cells. *Cell Death Differ* 2002; **9**: 626–635.
- 42 Qin L *et al.* Promoter attenuation in gene therapy: interferon-gamma and tumor necrosis factor-alpha inhibit transgene expression. *Hum Gene Ther* 1997; **8**: 2019–2029.
- 43 Smith HR *et al.* Recognition of a virus-encoded ligand by a natural killer cell activation receptor. *Proc Natl Acad Sci USA* 2002; **99**: 8826–8831.
- 44 Blake JA, Richardson JE, Davisson MT, Eppig JT. The Mouse Genome Database (MGD). A comprehensive public resource of genetic, phenotypic and genomic data. The Mouse Genome Informatics Group. *Nucleic Acids Res* 1997; **25**: 85–91.
- 45 Blake JA *et al.* MGD: the Mouse Genome Database. *Nucleic Acids Res* 2003; **31**: 193–195.
- 46 Havelkova H *et al.* T-cell proliferative response is controlled by loci Tria4 and Tria5 on mouse chromosomes 7 and 9. *Mamm Genome* 1999; **10**: 670–674.
- 47 Panoutsakopoulou V *et al.* Differences in the immune response during the acute phase of E-55+ murine leukemia virus infection in progressor BALB and long term nonprogressor C57BL mice. *J Immunol* 1998; **161**: 17–26.
- 48 Otto JM *et al.* Identification of multiple loci linked to inflammation and autoantibody production by a genome scan of a murine model of rheumatoid arthritis. *Arthritis Rheum* 1999; **42**: 2524–2531.
- 49 Butterfield RJ *et al.* New genetic loci that control susceptibility and symptoms of experimental allergic encephalomyelitis in inbred mice. *J Immunol* 1998; **161**: 1860–1867.
- 50 Silveira PA *et al.* Identification of the Gasa3 and Gasa4 autoimmune gastritis susceptibility genes using congenic mice and partitioned, segregative and interaction analyses. *Immunogenetics* 2001; **53**: 741–750.
- 51 McIndoe RA *et al.* Localization of non-Mhc collagen-induced arthritis susceptibility loci in DBA/1j mice. *Proc Natl Acad Sci USA* 1999; **96**: 2210–2214.
- 52 Daser A *et al.* Genetics of atopy in a mouse model: polymorphism of the IL-5 receptor alpha chain. *Immunogenetics* 2000; **51**: 632–638.
- 53 Bachy M, Bonnin-Rivalland A, Tilliet V, Trannoy E. Beta galactosidase release as an alternative to chromium release in cytotoxic T-cell assays. *J Immunol Methods* 1999; **230**: 37–46.
- 54 Ichikawa K *et al.* TRAIL-R2 (DR5) mediates apoptosis of synovial fibroblasts in rheumatoid arthritis. *J Immunol* 2003; **171**: 1061–1069.
- 55 Williams RW, Gu J, Qi S, Lu L. The genetic structure of recombinant inbred mice: high-resolution consensus maps for complex trait analysis. *Genome Biol* 2001; **2**: RESEARCH0046.
- 56 Williams RW, Gu J, Qi S, Lu L. Release 1 of the BXN Genotype Database: the genetic structure of recombinant inbred mice: high-resolution consensus maps for complex trait analysis. <nervenet.org/papers/bxn.html> 2001.
- 57 Taylor BA *et al.* Genotyping new B × D recombinant inbred mouse strains and comparison of B × D and consensus maps. *Mamm Genome* 1999; **10**: 335–348.
- 58 Laird PW *et al.* Simplified mammalian DNA isolation procedure. *Nucleic Acids Res* 1991; **19**: 4293.
- 59 Dietrich W *et al.* A genetic map of the mouse suitable for typing intraspecific crosses. *Genetics* 1992; **131**: 423–447.
- 60 Dietrich WF *et al.* A genetic map of the mouse with 4,006 simple sequence length polymorphisms. *Nat Genet* 1994; **7**: 220–245.

- 61 Lander E, Kruglyak L. Genetic dissection of complex traits: guidelines for interpreting and reporting linkage results. *Nat Genet* 1995; **11**: 241–247.
- 62 Churchill GA, Doerge RW. Empirical threshold values for quantitative trait mapping. *Genetics* 1994; **138**: 963–971.
- 63 Lynch M, Walsh B. *Genetics and Analysis of Quantitative Traits*. Sinauer: Sunderland, MA, 1998.
- 64 Belknap JK *et al*. Type I and type II error rates for quantitative trait loci (QTL) mapping studies using recombinant inbred mouse strains. *Behav Genet* 1996; **26**: 149–160.